Behavior of Reactive Powder Concrete Deep Beams

Prof. Dr. Hani M. Fahmi* Asst. Prof. Dr. Ihsan A.S AlShaarbaf**
Abdullah Sinan Ahmed**

Abstract

This investigation includes the behavior and shear strength characteristics of reactive powder concrete (RPC) deep beams subjected to concentrated loads. Seven reinforced deep beams made with RPC were cast and tested. The test variables included the shear span to effective depth ratio, and percentage of silica fume in the concrete. The effect of these parameters on the behavior of the test beams included deflection, concrete strains, failure mode, and ultimate loads were investigated.

The experimental results are compared with analytical results using the strut and tie model of ACI 318M-11 Code and found both results to be, in general, in good agreemsnt.

Keywords: Reactive Powder Concrete; Deep beams; Strut and Tie Model

* Al-Mansour University College
** Al-Nahrain University

1. Introduction

Reactive powder concrete (RPC) is an ultra-high strength, low porosity cementitious material with high cement and silica fume contents and low water/binder ratio, which is made possible with the aid of superplasticizers. In RPC, the absence of coarse aggregates is the major difference from conventional and high strength concretes. Compressive strengths greater than 200 MPa and modulus of rupture of 25-50 MPa with enhanced ductility and demandable durability may be achieved.

RPC is based on the principle that a material with a minimum of defects such as micro-cracks and inside voids will be able to achieve greater strength and enhanced durability. Hence, coarse aggregates are eliminated and the fine aggregates are replaced by fine sand with maximum particle size of approximately (600μm). The heterogeneity problems are substantially reduced with RPC and an improvement of the mechanical properties of the paste is gained through reduction in the aggregate /matrix ratio[5].

The design of reinforced concrete deep beams is a subject of considerable interest in construction practice. It has various structural applications ranging from pile-caps and wall foundations to transfer girders in tall buildings.

This paper describes an experimental work and analysis by the strut and tie model for RPC deep beams.

2.Experimental Program

The experimental program includes casting and testing control specimens and seven rectangular reactive powder concrete (RPC) deep beam specimens. The control specimens included 100x200mm cylinders for compression and splitting tensile tests and 280x70x70 mm prisms for the modulus of rupture test. The RPC deep test beams had 300 mm height, 110 mm width and 1400mm length. All the beams had a longitudinal steel ratio of 0.0244, consisting of four 16mm diameter deformed bars and a clear span of 1000 mm. The shear spans varied from 250 to 500 mm, resulting in five shear span/depth ratios, as shown in Table 1 and Figure 1.

All the RPC deep beams and associated control specimens were cast using mix proportions of (1 cement, 1 silica sand, 0.2 water by weight and 2% by volume of micro steel fibers), the silica fume ratios used were 15% of cement weight for specimen DB2, 20% for DB3, 25% for the rest of specimens.

The mixing procedure used was by mixing the desired quantity of silica fume in a dry state with the required quantity of cement. This process was continued for about 3 minutes, when ensuring that silica fume powder was thoroughly dispersed between cement particles, the fine sand was loaded into the mixer and mixed for 5 minutes. It was deemed necessary to have the granular materials pre-blended separately first. The pre-blended mix was loaded into the mixer. Then, the superplasticizer was dissolved in water and the solution of water and superplasticizer was added to the rotary mixer and all the mix ingredients were mixed for a sufficient time. Then the mixer was stopped and mixing was continued manually especially for the portions not reached by the mixer blades. The mixer was then operated for 5 minutes to attain reasonable fluidity. The steel fibers with length/dia. ratio of 52 were

added at the final stage of mixing (1 minute) and then the mixing process was continued for additional l5 minutes. The steel reinforcements was placed into the specially prepared steel beams molds before filling them and the control specimen's steel molds with the RPC prepared mix, vibrated and covered with plastic sheets for 24 hours. After which they were demolded and cured in water tanks for 27 days before testing.

The beams were gradually loaded by two-point load as shown in Fig. 1 until failure. Concrete strains and midspan deflections were measured and recorded during the tests. Concrete strains were measured by using demec points and an extensometer with 0.001 mm accuracy. Two sets of strain measurements were taken:

a) Compressive strains at the middle of the beam strut.
b) Tensile strains perpendicular to the beam strut.

The midspan deflections of the RPC beams were measured by using a dial gage with 0.01mm accuracy.

Table 1: Details of Deep Beam Specimens

Beam Specimen	shear span/depth	Steel fiber %	Silica fume %	A (mm)	B (mm)
DB1	**1.5**	**2.0**	**25**	**375**	**290**
DB2	**1.5**	**2.0**	**15**	**375**	**290**
DB3	**1.5**	**2.0**	**20**	**375**	**290**
DB4	**2.0**	**2.0**	**25**	**500**	**40**
DB5	**1.75**	**2.0**	**25**	**437.5**	**165**
DB6	**1.25**	**2.0**	**25**	**312.5**	**415**
DB7	**1.0**	**2.0**	**25**	**250**	**540**

A=Shear span B=Distance between loads

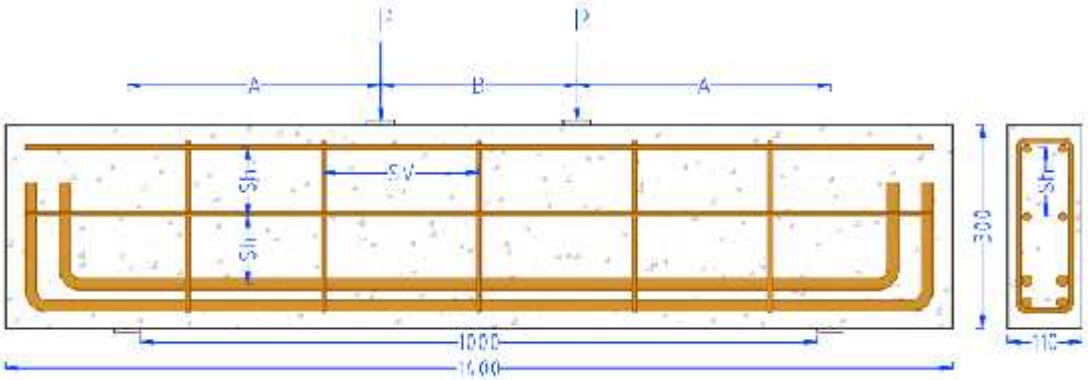

Figure 1: Details of specimen

3.Test Results and Discussion

3.1. Control Specimens

a) Compressive Strength:

Table 2 shows the effect of silica fume ratio on the compressive strength of concrete cylinders obtained using different mixes. This table shows that the cylinder compressive strength is increased by 13.96, 16.47% when the silica fume content is increased from 15% to 20% and from 15% to 25% as shown in Figure 2. This can be attributed to the enhancement of the microstructure and stronger bond between the steel fibers and the surrounding matrix with increasing silica fume content.

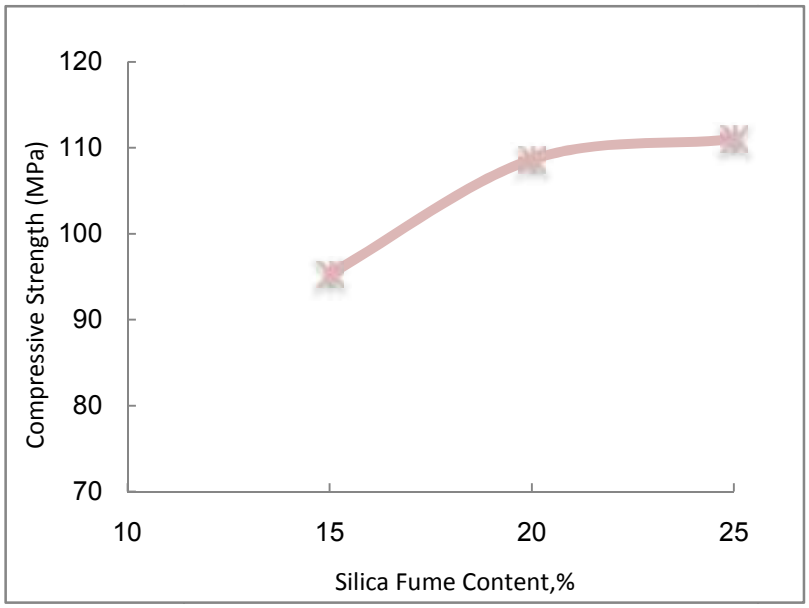

Figure 2: Influence of silica fume content on RPC compressive strength

Table 2: Effect of silica fume content on RPC compressive strength

Mix Designation	V_f %	Silica Fume %	Compressive Strength f'_c (MPa)	% Increase
M2.0-15	2.0	15	95.3	0 (Reference)
M2.0-20	2.0	20	108.6	13.96
M2.0-25	2.0	25	111.0	16.47

a) Splitting Tensile Strength:

Effect of silica fume content on splitting strength is similar to its effect on compressive strength. The effect of varying silica fume content is shown in Figure 3 and Table 3.

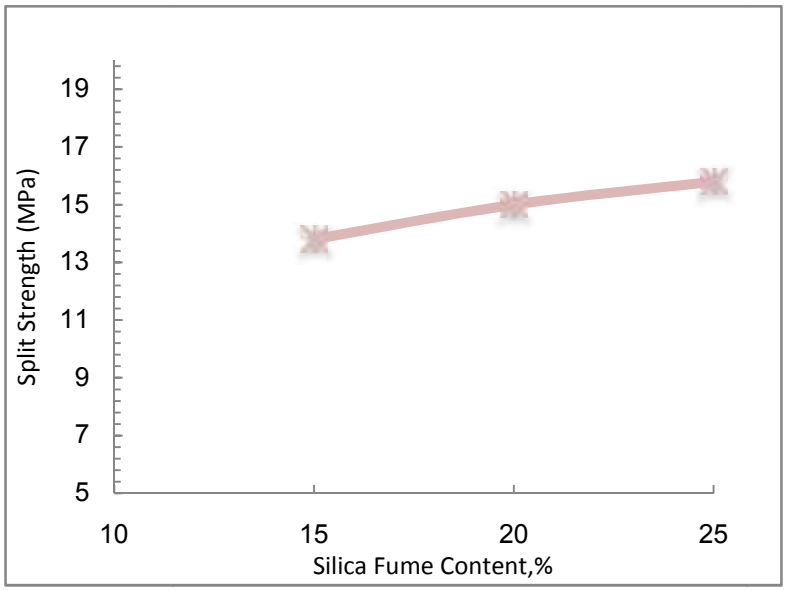

Figure 3: Influence of silica fume content on RPC tensile strength

Table 3: Effect of silica fume content on RPC tensile strength

Mix Designation	V_f %	Silica Fume %	Tensile Strength f_t (MPa)	% Increase
M2.0-15	2.0	15	13.8	0 (Reference)
M2.0-20	2.0	20	15	8.7
M2.0-25	2.0	25	15.8	14.5

a) Modulus of Rupture:

Modulus of rupture tests on RPC were carried out by using flexural tests in which a square prism is subjected to two points loading. Table 4 shows that the increase in the modulus of rupture due to increasing silica fume content from 15% to 20% is 10.46%. On the other hand an increase of 18.3% is achieved when the silica fume content is increased from 20% to 25%.

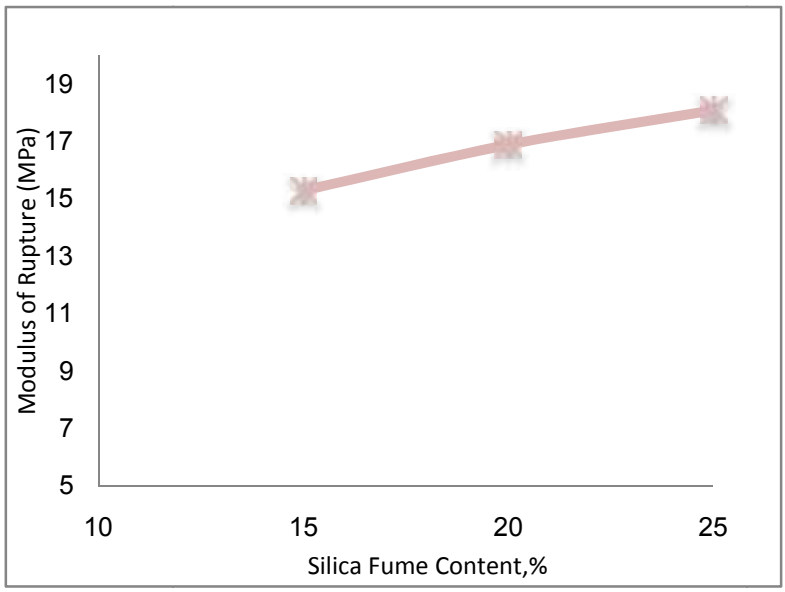

Figure 4: Influence of silica fume content on RPC modulus of rupture

Table 4: Effect of silica fume content on RPC modulus of rupture

Mix Designation	V_f %	Silica Fume %	Modulus of Rupture (MPa)	% Increase
M2.0-15	2.0	15	15.3	0 (Reference)
M2.0-20	2.0	20	16.9	10.46
M2.0-25	2.0	25	18.1	18.3

3.2. Deep Beam Specimens

The test results of the shear strengths of the first diagonal cracking and ultimate loads are shown in Table 5:

Table 5: Cracking and Ultimate Shear Strengths for Test RPC Beam Specimen

Beam Specimen	Concrete strength f'c MPa	Shear span/depth ratio	Silica Fume (%)	Diagonal Cracking Load (kN)	Ultimate Load (kN)	Failure Mode
DB1	111.0	1.5	25%	220	615	DT
DB2	108.6	1.5	20%	200	580	DT
DB3	95.3	1.5	15%	180	520	DT
DB4	114.9	2.0	25%	-	555	F
DB5	114.9	1.75	25%	-	490	F
DB6	106.1	1.25	25%	300	765	SC
DB7	106.1	1.0	25%	330	810	DT

* DT: diagonal tension failure, SC: shear-compression failure, F: flexural failure.

3.2.1. Failure Mode

Plate 1 shows the crack patterns after testing all the beams to failure. This plate shows that the failure mode for most of the deep beams tested was through a diagonal shear crack with different widths extending from the bottom of beam near the support to the loading points at the top with different widths. The cracks were accompanied, in some specimens, by the formation of new inclined cracks parallel to the initial cracks in the shear span. However, three specimens failed by flexural vertical cracks extended to the compression zone. The diagonal cracks extended towards the beam's bottom at or near the supports and the loading points at the top but did not reach both. The failure mode in these three specimens was changed because the specimens had high a/d ratio.

3.2.2.Effect of Shear Span to Effective Depth Ratio:

It is noticed from Table 5 that the increase of a/d ratio causes a decrease in the values of the shear cracking and failure loads, as shown in Figure 5.

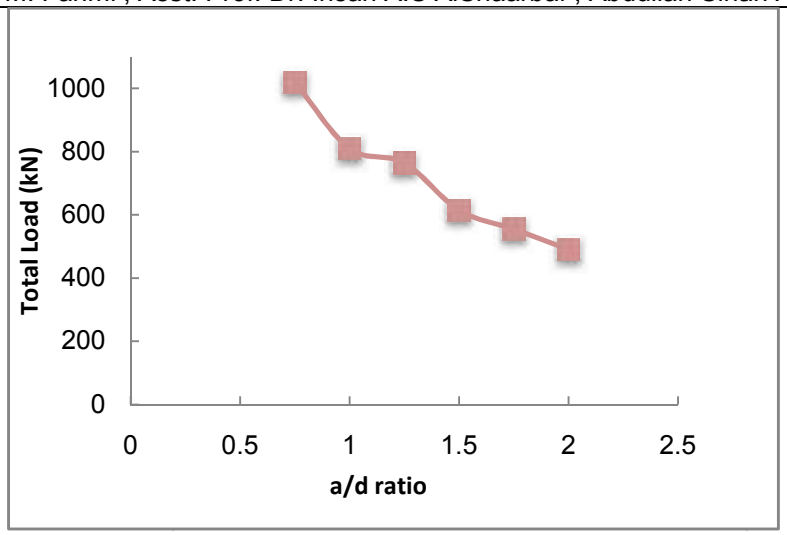

Figure 5: Effect of (a/d) ratio on the shear strength of RPC deep beams

a) Specimen (DB1)

b) Specimen (DB2)

c) Specimen (DB3)

d) Specimen (DB4)

e) Specimen (DB5)

f) Specimen (DB6)

g) Specimen (DB7)

Plate 1: Beam specimens after testing to failure

The failure mode of beam specimens 4 and 5 was by yielding of tensile reinforcement (flexural failure) and a diagonal tension failure is observed in the other beam specimens. Excluding the specimens that failed in flexure, an increase in the ultimate shear strength of 24.4%, 31.7% is obtained in the ultimate shear strength when the a/d ratio decreased from 1.5 to 1.25, and 1.0 respectively.

3.2.3 Effect of Silica Fume Percentage (SF)

It can be seen from Table 5 that for a/d= 1.5 and V_f=2.0% increasing the SF from 15 to 20 and 25%, the diagonal cracking load is increased by 11.1 and 22.2%, respectively. Also, the ultimate load is increased by 11.5 and 18.3%, respectively, as shown in Figure 6.

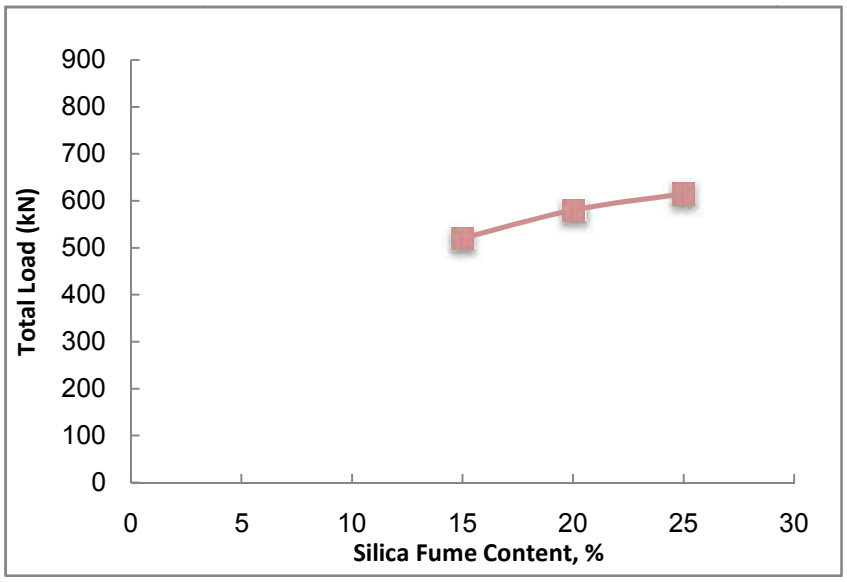

Figure 6: Effect of silica fume content on the shear strength of RPC deep beams

3.2.4.Load-mid deflection Relationships

From the load-midspan deflection relationship shown in Figure 7 and 8 for all RPC beams, the following three distinct stages are observed:

1. The first stage shows linear behavior with constant slope.

2. In the second stage, vertical flexural cracks were initiated at the tensile face within the maximum bending moment region of the beam, and extend upward, then inclined cracks originated in the shear spans. These cracks developed with increased load, causing a corresponding shift of the neutral axis towards the compression face, and consequently, a continuous reduction in the moment of inertia of the cracked section. The curve changed from linear to non-linear behavior in this stage.

3. In the third stage, the shape of the load-deflection curve tends to be asymptotic to the horizontal as the beam approached its ultimate load.

It can be observed from Figure 7 that at the early stages of loading, the deflections are almost identical for all beams. The a/d ratio is the only parameter which affects the initial deflections through controlling midspan bending moment values. Hence, the deflection for a given load increases with the increase of a/d ratio.

Figure 8 depicts the effect of silica fume content on the load-deflection behavior. It is clear from this figure that for a given load, the deflections are slightly decreased

with the increase in SF content. This is related to the enhanced particle packing density and intensive chemical reaction due to pozzolanic reaction with silica hydrate conversion which leads to increased RPC strength and modulus of elasticity. Therefore, any increase in SF content enhances the crack control and decreases deflection of the RPC beam for a given load. For a load of 460kN, decreasing SF from 25% in DB1 to 20% in DB2 and 15% in DB3 results in an increase in their deflections by 8% and 33.5%, respectively when compared with those of DB1.

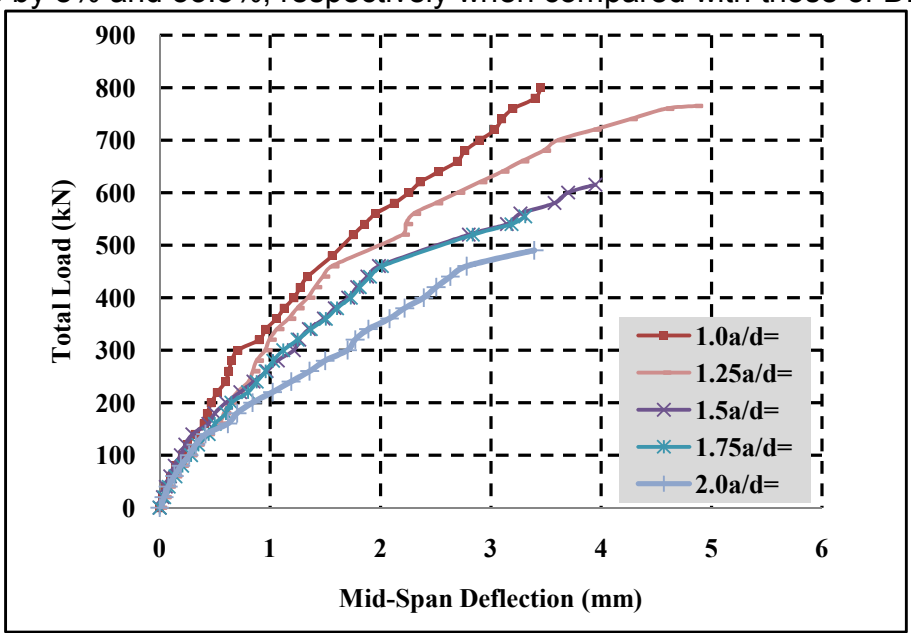

Figure 7: Effect of a/d ratio on mid-span deflection

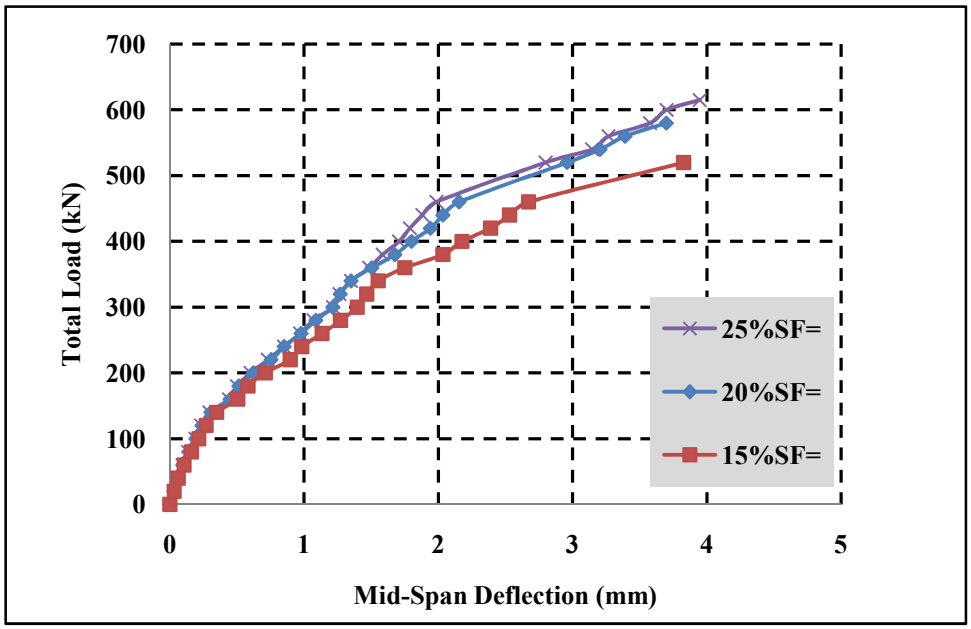

Figure 8: Effect of silica fume content on mid-span deflection

3.2.5.Concrete Strain:

Generally, for the beams that failed in shear, maximum strains were measured along the struts connecting the applied load point and the supports.

Figures 9 to 15 show the concrete strains behavior in the compression and tension zones of RPC beams. A comparison of each test variable is shown in Figures 16 to 19.

3.2.5.1Effect of a/d Ratio:

The effect of a/d ratio becomes noticeable after the formation of the first inclined shear crack. Tensile strains in the concrete decrease as the a/d ratio decreases, which indicates that the beam specimens show stiffer behavior and larger resistance to the formation of diagonal shear cracks. All the concrete tensile curves consist of two parts, the linear and nonlinear parts. It is noticed that the linear part covers a higher load range as the a/d ratio decreases in the tested beams.

3.2.5.2 Effect of Silica Fume

It can be observed From Figures 16 and 17 that the silica fume content has a noticeable effect on the strain values of concrete. Generally, for a given load level, the RPC beam with larger amount of silica fume undergoes smaller surface strain (i.e. stiffer beam).

During the tests, the following interesting points were noticed:

1. At the early stages of loading and the formation of flexural cracks, the concrete strains at the strut position are insignificant which reflect the fact that the formation of flexural cracks has insignificant effect on the strain of the concrete strut.
2. As the load is increased, the compressive strain increases linearly. When shear cracks begin to develop near and at the middle of the inclined strut due to the tensile force at that location, the readings of the concrete tensile strain show a sudden increase due to the propagation of cracks. This behavior can clearly be noticed in the tensile strain diagrams of all the tested beam specimens that failed in shear.

The sudden changes in the concrete tensile strain values decrease as the failure mode changes from shear to flexural.

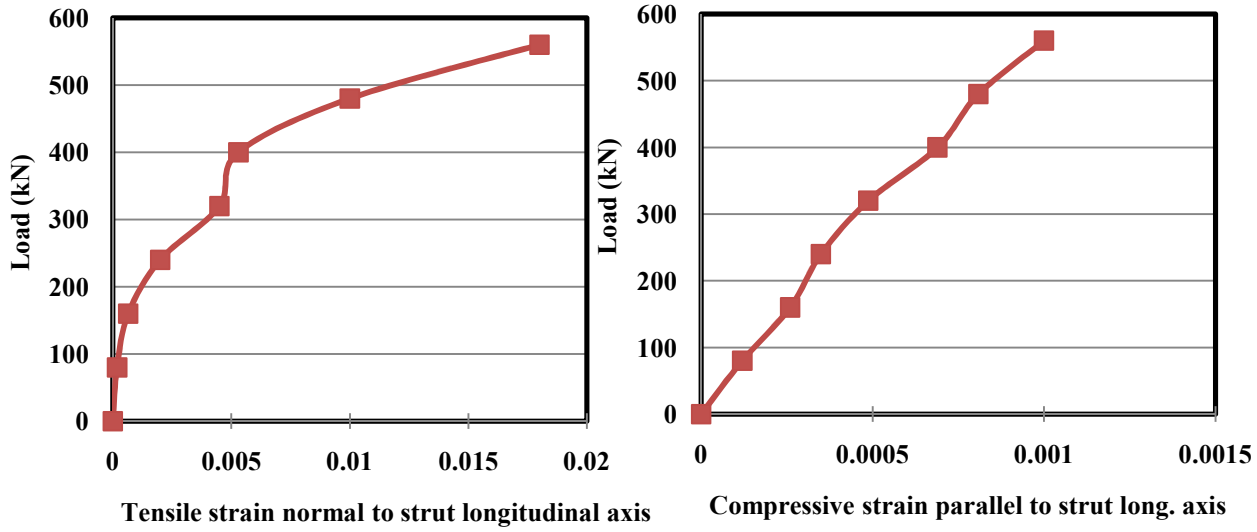

Figure 9: Load versus concrete strains for deep beam DB1

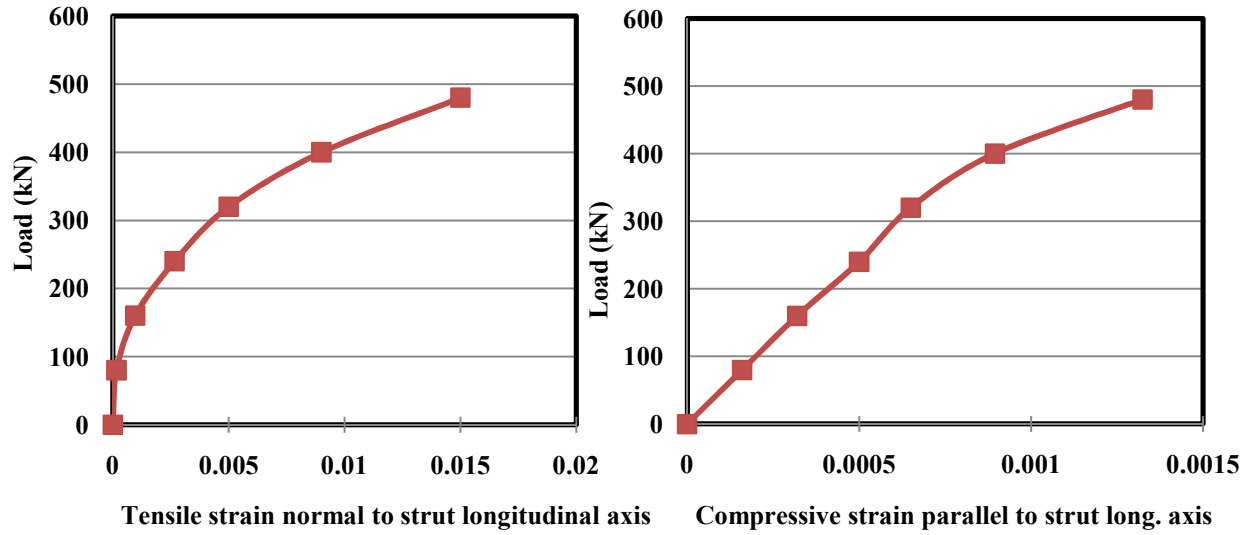

Figure 10: Load versus concrete strains for deep beam DB2

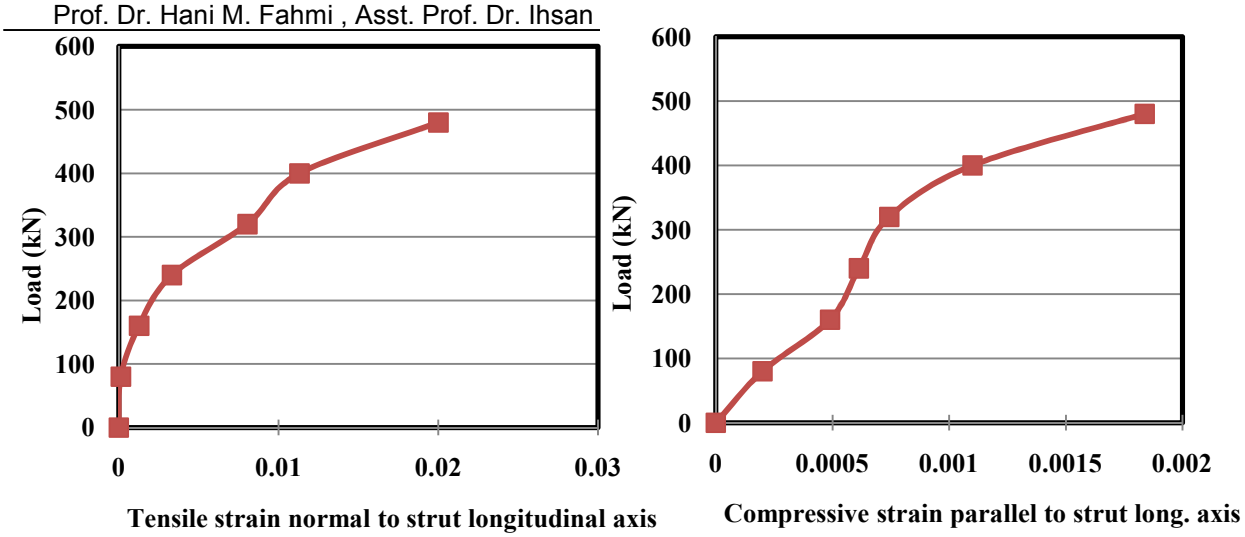

Figure 11: Load versus concrete strains for deep beam DB3

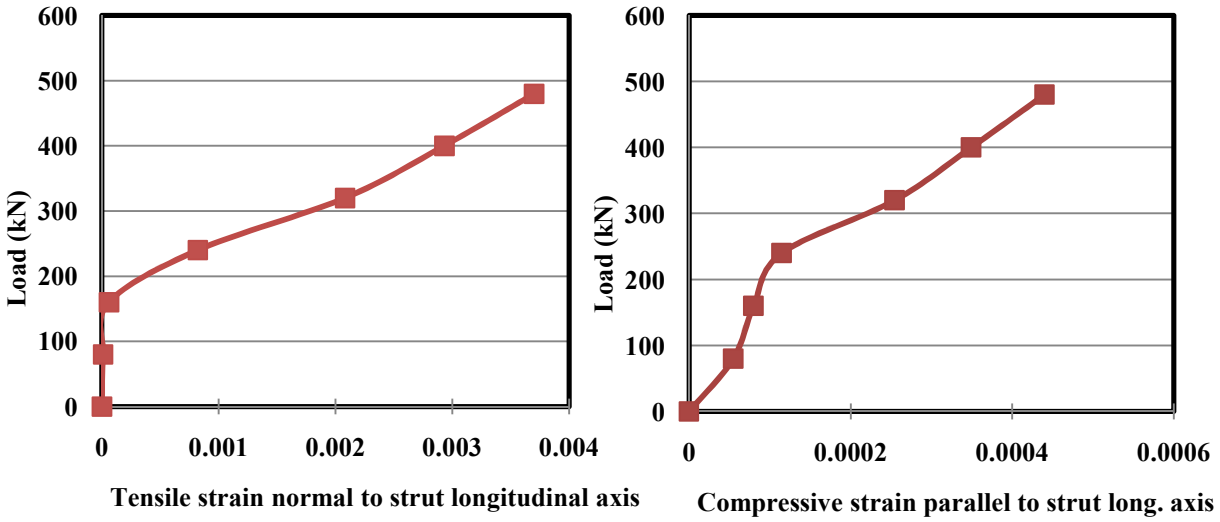

Figure 12: Load versus concrete strains for deep beam DB4

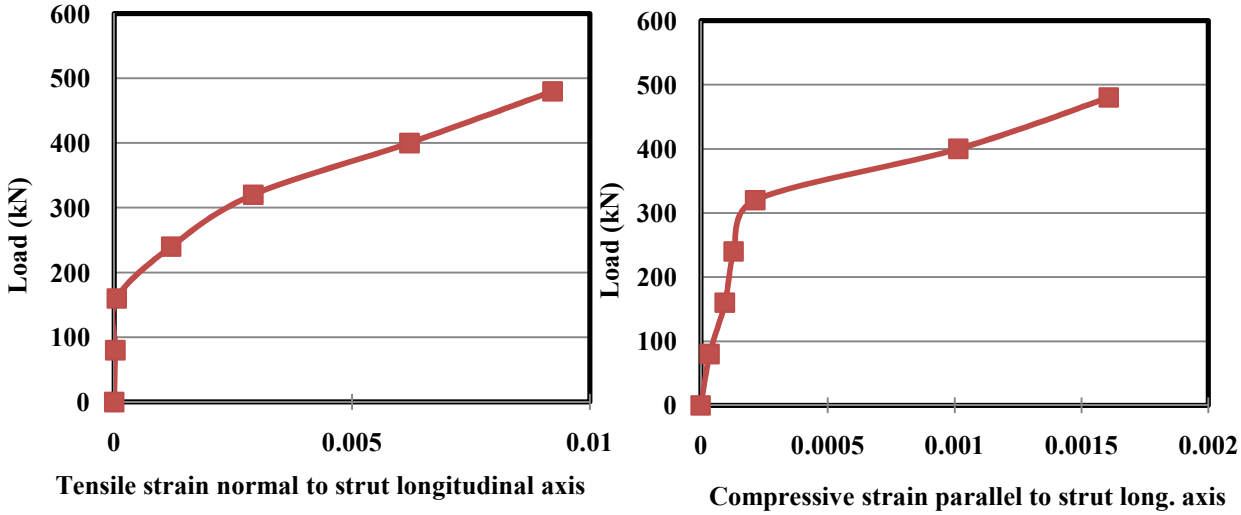

Figure 13: Load versus concrete strains for deep beam DB5

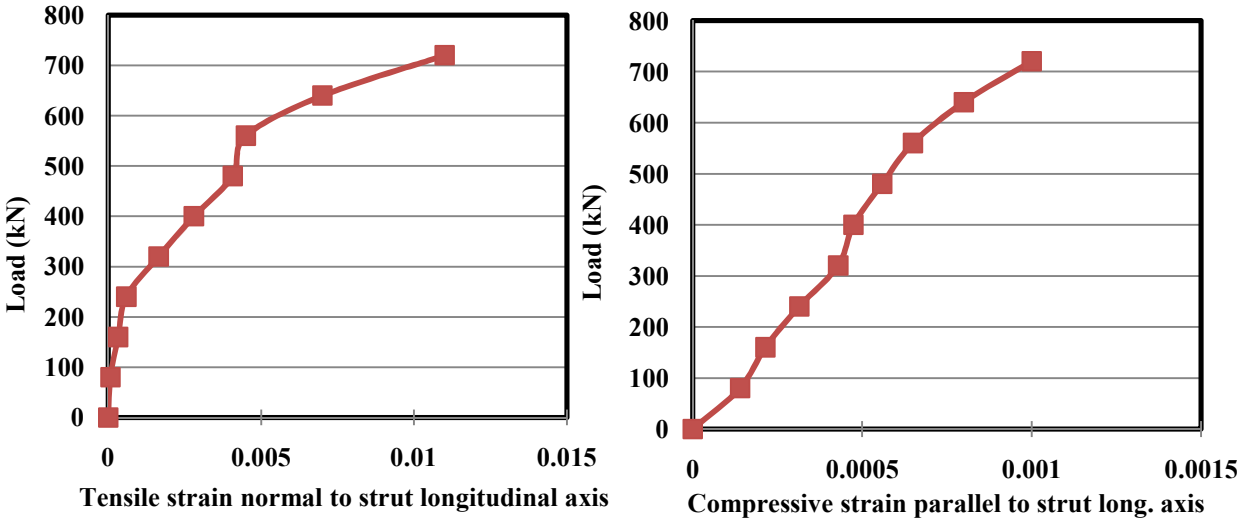

Figure 14: Load versus concrete strains for deep beam DB6

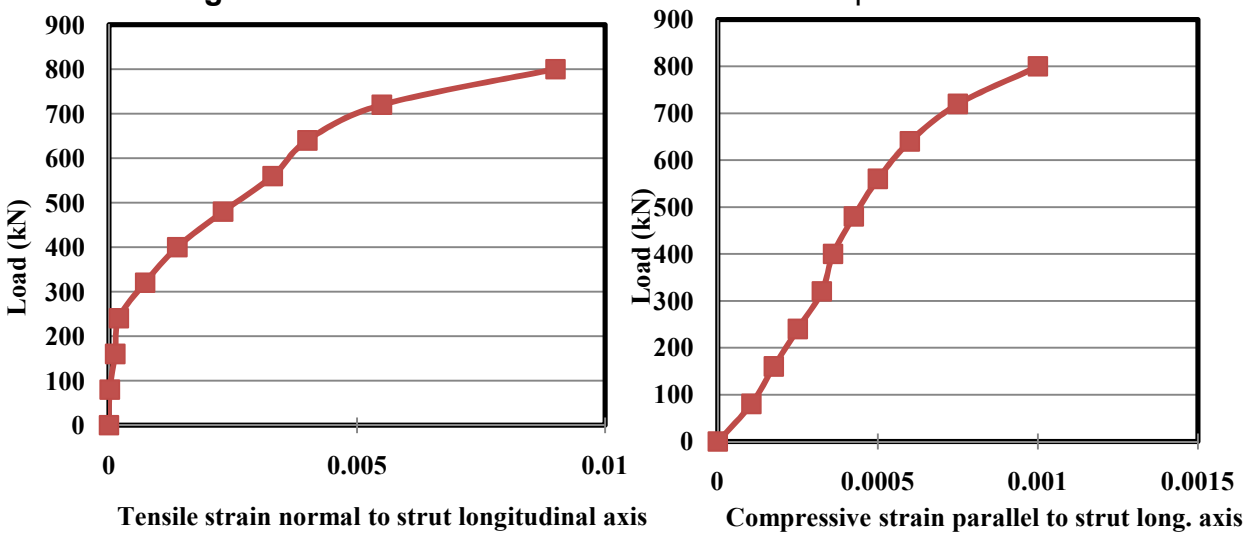

Figure 15: Load versus concrete strains for deep beam DB7

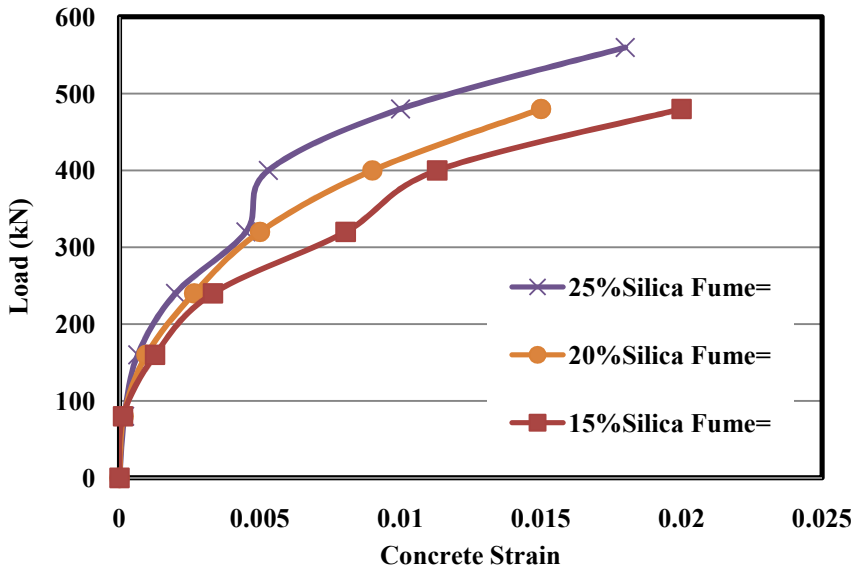

Figure 16: Effect of silica fume content on load-compressive concrete strain (parallel to strut axis)

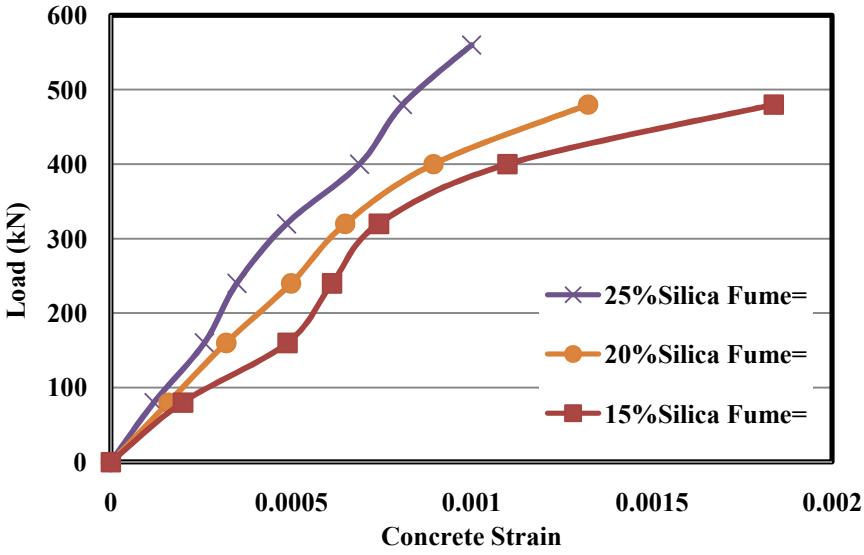

Figure 17: Effect of silica fume content on load-tensile concrete strain (normal to strut axis)

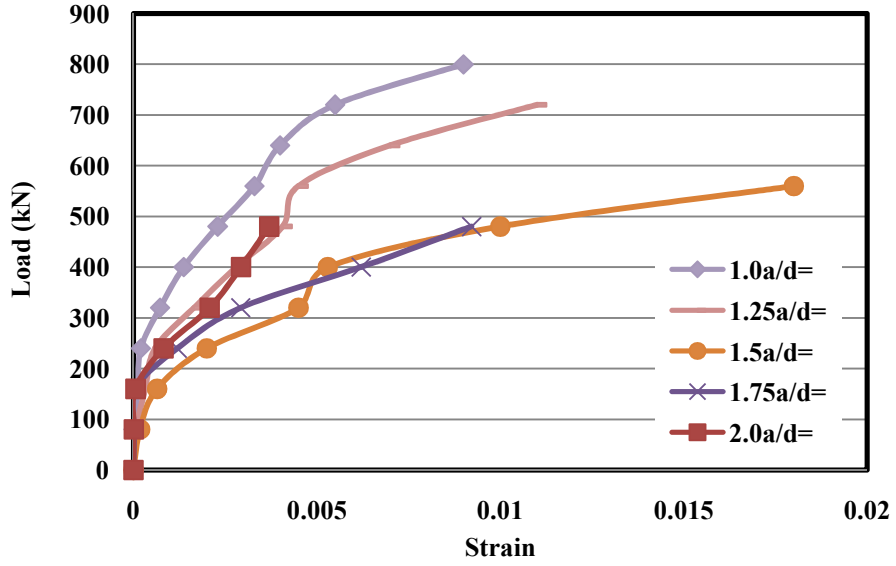

Figure 18: Effect of a/d ratio on load-compressive concrete strain (parallel to strut axis)

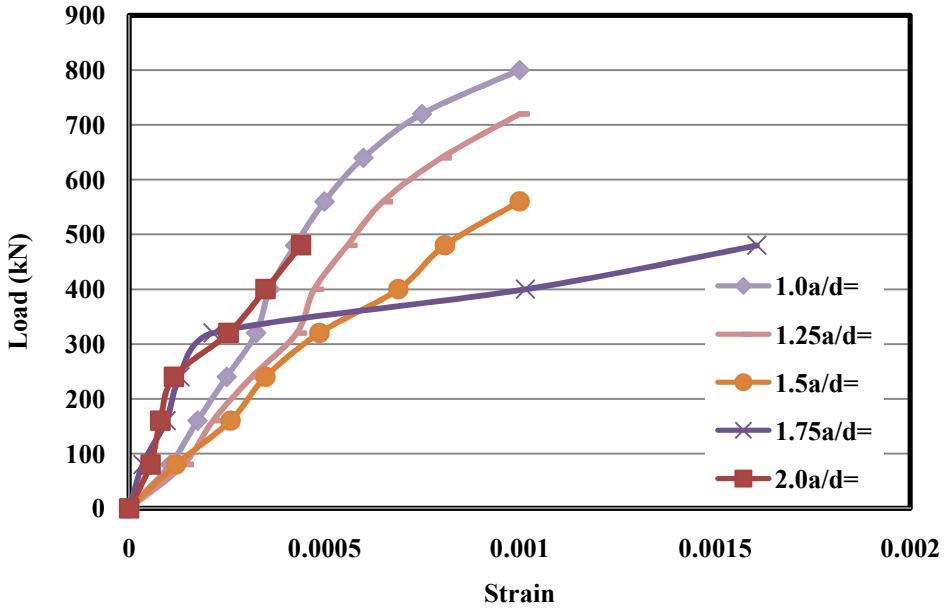

Figure 19: Effect of a/d ratio on load-tensile concrete strain (normal to strut axis)

4. Strut and Tie Model for RPC Deep Beams

In deep beams without web reinforcement, the shear force is resisted primarily by the strut forming between the loading point and the support. For beams in which flexural, bearing and anchorage failures are prevented, the shear capacity is governed by the compressive capacity of the strut, which is a function of the strut dimensions. The strut is usually assumed to be a bottle shaped strut. A simple idealization of the shape of strut is adopted as shown in Figure 20.

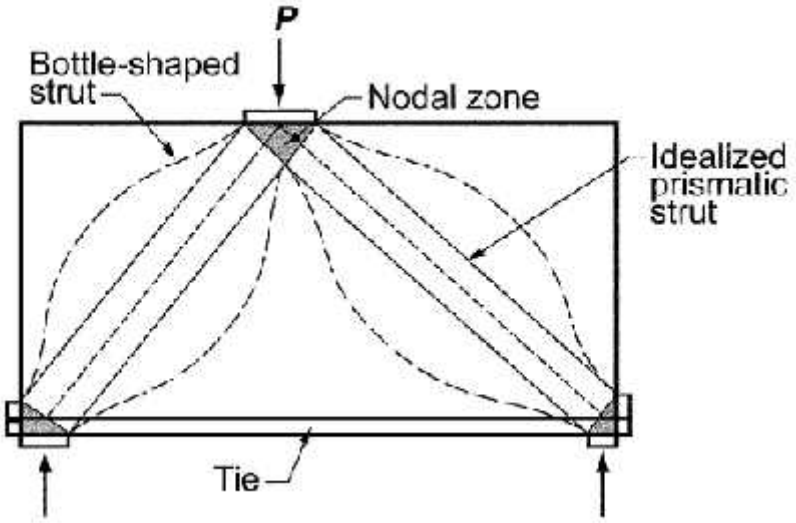

Figure 20: Shape of strut(1)

According to ACI 318M-11 Code, the nominal compressive strength of a strut should be taken as:

$$F_{ns} = f_{ce} A_{cs} \quad \text{… (1)}$$

where,

A_{cs} = area of strut.

f_{ce} = compressive stress in the strut given by:

$$f_{ce} = 0.85 \beta_s f'_c \quad \text{… (2)}$$

where,

β_s = 0.60 for strut without web reinforcement.

β_s = 0.75 for strut with web reinforcement satisfying (Figure 21):

$$\rho_p = \sum \frac{A_{si}}{b_s s_i} \sin \alpha_i \geq 0.003 \quad \text{… (3)}$$

where,

A_{si} = total area of surface reinforcement at spacing s_i in the *i*-th layer crossing a strut, with reinforcement at an angle α_i to the axis of the strut.

b_s = width of strut

α_i = angle between *i*-th layer of reinforcement and axis of strut

s_i = spacing of reinforcement in *i*-th layer

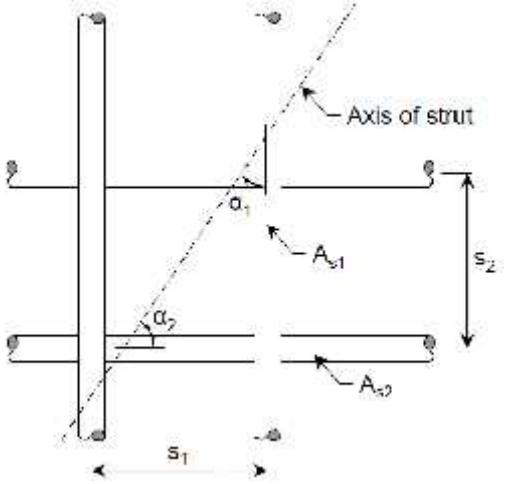

Figure 21 : Calculation of web reinforcement in ACI 318-11

The strut and tie model is applied to the tested RPC beams , the results shown in Table 6 indicates that the ACI strut strength computed results is lower values than the experimental, the predicted values are enhanced when using ACI equations with web reinforced strut.

Table 6: Experimental and predicted failure loads using ACI recommendations

Beam No.	Experimental failure load kN (1)	Predicted		Ratios	
		ACI without web reinf. β_s = 0.6 (2)	ACI with web reinf. β_s = 0.75 (3)	(2)/(1)	(3)/(1)
DB10	615	454	569	0.738	0.925
DB11	580	437	549	0.753	0.947
DB12	520	388	487	0.746	0.937
DB13	490	356	447	0.727	0.912
DB14	555	400	503	0.721	0.906
DB15	765	494	619	0.646	0.809
DB16	810	562	705	0.694	0.870
			Average	**0.718**	**0.901**

4. Conclusions

From the experimental and computed results in this investigation on the behavior of reactive powder deep beam concrete beams, following conclusions are made:

1. The shear span/effective depth ratio (a/d) has a significant effect on the shear strength of RPC deep beam and determines the mode of failure. An increase in the ultimate shear strength of 24.4 and 31.7% is obtained when the a/d ratio decreased from 1.5 to 1.25, and 1.0 respectively

2. Increasing silica fume (SF) content from 15 to 20 and 25% increases the shear strength by 11.5 and 18.3%, respectively. This is attributed to the fact that the increase SF in the RPC matrix enhances particle packing, which leads to improving the microstructure of RPC matrix and increases RPC strength.

3. The predicted RPC deep beam strengths using the ACI strut and tie model are underestimated in comparison with the experimental values by up to about 28%.

4. Using a reduction factor of β = 0.75 results in improved prediction values of the shear strengths of RPC deep beams, with a reduced maximum difference between the experimental and computed values of only 10%.

Symbols

RPC= Reactive Powder Concrete.

DB= Deep Beam Specimen

a= Shear span (the horizontal distance between the centerlines of support and load), mm

d= Effective depth, mm

V_f= Steel fiber content in the RPC mix, %

SF= Silica Fume content in the RPC mix, % of cement weight

References

1. ACI 318M-11, "**Building Code Requirements for Structural Concrete and Commentary**", American Concrete Institute, Farmington Hills, Michigan, 2011.
2. Richard, P., and Cheyrezy, M., "**Reactive Powder Concrete with High Ductility and 200-800 MPa Compressive Strength"**, ACI SP144-24, January1994, pp. 507-518.
3. Schlaich, J., Schafer, K., and Jennewein, M., **"Toward a Consistent Design of Structural Concrete"**, PCI Journal, Vol. 32, No.3, May- June 1987, pp. 74-150.
4. Warwick, W.B., and Foster, S.J., "**Investigation into the efficiency factor used in non-flexural reinforced concrete member design"**, UNICIV Report No. R-320, School of Civil Engineering, University of New South Wales, July 1993, 81 pp.
5. Warnock, R., **"Short-Term and Time-Dependent Flexural Behavior of Steel-Fiber Reinforced Reactive Powder Concrete Beams"**, PhD. Thesis, University of New South Wales, 2005, 201 pp.
6. Stephen, J., Foster, B.E., and Ian Gilbert, B.E., "**Tests on High Strength Concrete Deep Beams",** School of Civil Engineering, University of New South Wales, June 1996. 56 pp.

تصرف العتبات العميقة المصنوعة من خرسانة المساحيق الفعالة

ا.د. هاني محمد فهمي* ا.م. د.احسان علي صائب الشعرباف **

م.م.عبدالله سنان احمد**

المستخلص

يتضمن هذا البحث تصرف ومقاومة القص للعتبات العميقة المصنعة من خرسانة المساحيق الفعالة تحت تأثير احمال مركزّة.تم اعداد وفحص سبعة عتبات عميقة وتم دراسة تاثير نسبة فضاء القص الى العمق الفعال للعتبات ونسبة السلكا الفعالة في الخرسانة.وتم ايضاً دراسة تاثير هذين المتغيرين على تصرف عتبات الأختبار الذي شمل الهطول، انفعال الخرسانة ، نوع الفشل والحمل الأقصى لها . تمت كذالك مقارنة النتائج المختبرية لمقاومة العتبات مع نتائج تحليلية باستخدام نموذج الأنضغاط- الشد في مدونة الخرسانة الأمريكية ACI 318M – 11 وكانت النتائج متوافقة بشكل عام .

*رئيس قسم الهندسة المدنية- كلية المنصور الجامعة
** جامعة النهرين